

Proposing a circular economy for mine tailings: using them as catalysts in the treatment of landfill leachate

Rodrigo Poblete^{a*}, Vicente Salinas^b, Manuel I. Maldonado^{c,d}

^a Universidad Católica del Norte, Facultad de Ciencias del Mar, Escuela de Prevención de Riesgos Y Medioambiente, Coquimbo, Chile

^b Instituto de Ciencias de la Ingeniería, Universidad de O'Higgins, Rancagua, Chile.

^c CIEMAT-Plataforma Solar de Almería, Ctra. De Senes s/n, 04200, Tabernas, Almería, Almería, Spain

^d CIESOL, Joint Centre University of Almería-CIEMAT, 04120 Almería, Spain.

*Corresponding author: rpobletech@ucn.cl

Abstract

Mine tailings (MT), a significant by-product of the mining industry, pose environmental risks due to their metal content and social hazards when they are located near urban areas. However, their mineral composition, rich in feldspars, quartz, phyllosilicates, and TiO₂, offers potential for reuse within a circular economy framework. In this context, this study evaluates the catalytic application of MT in a sonophotocatalytic process to treat mature landfill leachate (LL), a recalcitrant effluent with low biodegradability. Using a full factorial design, the effects of catalyst load, hydrogen peroxide concentration, and pH of the solution on the removal of total organic carbon (TOC), Chemical Oxygen Demand and aromatic compounds (Abs₂₅₄) of the landfill leachate were assessed. Optimal conditions (2000 mg/L MT, 3000 mg/L H₂O₂, pH 3) led to 29.8% and 50.2% removal of TOC and aromatic compounds, respectively. Under these optimized physicochemical conditions applied for 3 hours of treatment, the removal of TOC, COD, and aromatic compounds was 84.9%, 69.6%, and 88.7%, respectively.

The biodegradability of treated landfill leachate improved significantly, exceeding 80% in the Zahn-Wellens test, with no detectable leaching of metals from the catalyst. These findings demonstrate the feasibility of repurposing MT as photocatalysts for landfill leachate treatment, offering a sustainable solution to two pressing waste streams.

Keywords: Sonophotocatalysis; Advanced Oxidation Processes; Biodegradability Enhancement; Zahn-Wellens Test.

1. Introduction

One of the most important economic activities of Chile is mining (Zhang and Schippers, 2022), where the exportations of copper, gold, and iron are very important. However, this industrial activity generates solid waste known as MT (Malafeevskiy et al., 2025; Campos-Medina et al., 2023), which are a combination of rocks and fluids from concentrators, washeries and mills, resulting from the extraction of metals from the mines (Texeira et al., 2023). In Chile, there are currently 765 dams, 22.6% of which are abandoned, for instance, in Andacollo, located in the Coquimbo region, tailing piles are very noticeable. These solid wastes, generated during the production of gold and copper, are an important aspect of the landscape due to their urban locations very close to the inhabitants of this city (Vega et al., 2022); (Leiva G. and Morales, 2013).

These MT contain unrecovered and moderately economically relevant amounts of metals (Zhang and Schippers, 2022), considered waste (Marín et al., 2020). The presence of metals in soils poses environmental risks due to their toxicity, accumulation, and persistence (Luo et al., 2012), which may affect the population (Vega et al., 2022). Metals are transported due to the action of erosion by water and wind or acid drainage, negatively affecting the environment (Vega et al., 2022) and disturbing the metabolisms of the microorganisms in the soil where the tailing is (Mao et al., 2024). MT have been found in urban areas, which could impact the population (Moya et al., 2019). Therefore, adequate MT management is transcendental for environmental, economic, social, and other reasons (Botero et al., 2024; Campos-Medina et al., 2023).

However, these MT can contain constituents with interesting properties that can be used as catalysts for the advanced oxidation processes, in wastewater treatment, thus supporting a circular economy. The presence of substances such as titanium, iron oxides, copper, and silica, among others, makes them suitable as potential photocatalysts in photo-Fenton and ultrasound processes to treat complex wastewater, such as LL (Poblete et al., 2024a). The use of a catalyst enhances pollutant removal; nevertheless, the load must be optimized since further increments can have a negative effect on the photocatalysis due to the cluster of particles and the decrease in the light pathway (Tekin et al., 2022).

LL is generated through the percolation of water from the wet municipal waste and rainfall as it filters through the layers of the landfill, reacting chemically and biologically, obtaining a liquid that presents high amounts of complex and recalcitrant substances, such as dissolved organic matter, chemical oxygen demand (COD), total organic carbon (TOC), heavy metals, phenols, and halogenated compounds (Wdowczyk et al., 2025; Naveen et al., 2017).

Applying biological treatments is efficient for young LL because of its biodegradability characteristics. Nevertheless, old and mature LL are not biodegradable due to the presence of toxic compounds, which impede this kind of treatment (Kwarciak-Kozłowska and Fijałkowski, 2021; Seibert et al., 2019). LL is a complex and resistant wastewater with very high concentration of in organic matter, generated during the

decomposition of municipal solid waste in sanitary landfills (Mohammad et al., 2022), being typically characterized by highly concentrated dark color (Jagaba et al., 2021) and elevated levels of dissolved organic matter and salts, along with poor biodegradability (Keyikoglu et al., 2021). In fact, LL is considered much more polluted than the municipal wastes water due to its toxic constituents such as pesticide, phenols and halogenated compounds, nitrogen compounds and organic and inorganic xenobiotics (Kirilova et al., 2025) .

Due to their characteristics, old LL are a source of pollution, the landfilling must be secured with an adequate cover system to avoid the infiltration of the LL (Min et al., 2024) and the LL must be adequately treated (Lei et al., 2023; Joshi and Gogate, 2019).

Conventional treatment systems for LL are based on the use of membrane filtration, ozonation, activated carbon adsorption, and advanced oxidation processes (AOP) (Almeida-Naranjo et al., 2023; Rout et al., 2021). These technologies, especially adsorption, stand out for their simplicity, low cost, and high effectiveness against emerging contaminants (Almeida-Naranjo et al., 2023). Similarly, membrane separation methods such as nanofiltration, ultrafiltration, and reverse osmosis have shown high potential for their removal (Kirilova et al., 2025). AOPs, classified according to their energy source (chemical, UV or electrochemical), enable the efficient degradation, due oxidation, of xenobiotic compounds, with reports of nearly 100% removal for drugs such as doxycycline, ciprofloxacin and ibuprofen (Arvaniti et al., 2022).

AOPs effectively depurate toxic organic wastewater. For instance, the use of non-thermal plasma, technology applied to generate oxidant radicals to depurate LL that reduces organic matter and metals in this kind of wastewater (Seid-mohammadi et al., 2021).

Other of the most interesting alternatives to be applied in LL is the photo-Fenton process (Singa et al., 2023). It is a homogeneous photocatalytic process, where Fe^{2+} ions react with hydrogen peroxide under UV irradiation, generating the powerful oxidant (HO^{\bullet}) and Fe^{3+} ions, and this Fe^{3+} , after that reacts with hydrogen peroxide, generating Fe^{2+} ions and hydroperoxyl, radical (HO_2^{\bullet}), that is a weaker radical (Kösem et al., 2024).

Another important AOP used to oxidise organic contaminants present in water is the interaction between TiO_2 and UV irradiation. When the surface of this semiconductor is irradiated with UV photons, electron-hole pairs are produced, which trigger redox reactions due to the excitation of electrons from the valence band (VB) to the conduction band (CB) (Jari et al., 2025), producing hydroxyl radicals (HO^{\bullet}) and superoxides ($\text{O}_2^{\bullet-}$).

The ultrasound process (US) is also an AOP and an interesting method to produce oxidant radicals in water. One of its key mechanisms is acoustic cavitation in the

inertial regime. This phenomenon occurs when high-intensity ultrasound waves propagate through a liquid, causing the formation, growth, and violent collapse of microbubbles. The implosion of these bubbles generates extreme localised conditions- temperatures of thousands of kelvins and pressures of several hundred atmospheres- enabling pyrolytic reactions and the generation of reactive radical species such as hydroxyl radicals (HO•) (Rayaroth et al., 2016). This process offers several advantages, such as improving mass transfer, enhancing turbulence and mixing, and improving catalytic efficiency (Sheik Moideen Thaha and Sathishkumar, 2025). Ultrasound irradiation in water generates small cavities with the gases dissolved in the water, which implode, producing conditions of high temperature and pressure, causing a pyrolytic cleavage of water molecules, generating H• and HO• (Su et al., 2024). As can be seen in reactions 1-4, it produced H₂O₂ and HO₂• under US irradiation:



US}} represents ultrasound irradiation.

Also, the abrupt collapse of the bubble due to US irradiation emits picosecond flashes of UV irradiation (Hiller et al., 1994), called bubble sonoluminescence, that can be taken advantage of for the degradation of organic pollutants (Gareev et al., 2023), via direct photolysis or photo-Fenton process, because it can be produced in the bulk of the polluted water, minimizing the scattering effect caused by colloids or turbidity in the water, very relevant in LL, even after filtration and coagulation/flocculation processes (Alanís et al., 2025).

Another potential application of the US process is in combating *Helicobacter pylori*. Following ultrasound exposure, singlet oxygen is generated, which contributes to bacterial elimination by disrupting biofilms and enhancing the removal of intracellular bacteria through the stimulation of autophagy (Yin et al., 2025).

US can also be used in welding processes, for example, Ultrasonic spot welding of copper foils (O–Cu) was improved by using a surface gradient structure, which generated a nanocrystalline layer with lower friction. This increased mechanical strength and welding temperature and modified the fracture mechanism, replacing cleavage with micro-pits (Ni et al., 2025).

Although advanced oxidation processes such as photo-Fenton and US are widely used to treat complex wastewaters, challenges such as high operational costs, limited catalyst efficiency, and the need for high energy inputs remain. Despite the environmental risks posed by MT, no study has investigated their catalytic potential

in wastewater treatment, making this work the first to explore this approach. Our study proposes an innovative approach to address both environmental concerns associated with MT and treating persistent organic pollutants in LL.

Circular economy strategies promote the use of waste as an input to generate value a second time or several times and extract valuable substances as metals (Nesterov et al., 2024). For instance, wastes as MT are a source of rare earth elements that can be incorporated in economic processes (Lima et al., 2022). In this context, approaching MT from a circular economy perspective represents a significant opportunity to reduce environmental impacts and increase the value of materials generated during extraction and processing operations (Tayebi-Khorami et al., 2019). The revalorisation of MT may promote the circular economy and waste reduction by transforming these materials from hazardous waste into valuable resources for environmental remediation.

Therefore, this study contributes to the dual goals of reducing environmental pollution and enhancing resource efficiency in the mining industry by performing a factorial design to determine the importance of the factors evaluated.

Considering that, in the best-known of the authors, there are no published studies that have used MT as a catalyst to depurate wastewater, this is the first study aimed at applying MT as a photocatalyst to evaluate this in the treatment of landfill leachate, performing a factorial design to determine the importance of the factors evaluated.

Unlike previous studies that have used modified industrial materials or commercial catalysts such as TiO_2 , our work explores the direct use of mining tailings without prior structural modification as active catalysts in a sonophotocatalytic process to treat mature landfill leachates.

Given that MT contain minerals with adsorbent and catalytic properties, the hypothesis of this study is that these can be used as effective catalysts in sonophotocatalytic processes to increase the degradation of organic pollutants and the biodegradability of mature landfill leachates, without causing metal leaching. This study evaluates, for the first time, this application of the MT under a factorial design that considers catalyst load, H_2O_2 concentration and pH as critical factors.

Therefore, an ultrasound process coupled with a photocatalytic process, with different loads of MT, concentrations of H_2O_2 , and pH of the solution, was applied to study the removal of pollutants present in a LL.

2.- Materials and methods

2.1- Sample Collection

195 50 kg of MT was obtained from Andacollo City, (30° 14' 14" S, 71° 5' 1.79" W), Chile,
196 where the tailing is very near the population, as can be seen in the photographs
197 presented in Figure 1. The sample was taken to the Universidad Católica del Norte
198 and stored in a closed container in the dark, before characterisation and
199 experimentation.



Fig. 1. Photographs of the MT obtained from Andacollo.

2.2.- Catalyst Characterization

The characterisation of the MT was performed using X-ray diffraction (XRD) and quantitative evaluation of minerals by scanning electron microscopy (QEMSCAN), and the equipment was an X-ray Diffractometer Bruker model D8 Advance and goniometer Vertical Bragg-Brentano radiation Cu Ka1 ($\lambda = 1.5406 \text{ \AA}$).

The MT was mainly composed of Feldspars (Plagioclase Series), Quartz (SiO₂), Biotite/Phlogopite, Muscovite/Sericite, Cu-bearing Phyllosilicates, Montmorillonite, and TiO₂ rutile phase, with a mass percentage composition of 36.43, 15.61, 7.57, 7.40, 5.58, 3.38, and 0.39, respectively. Figure 2 shows the X-ray diffraction (XRD) and quantitative evaluation of minerals by scanning electron microscopy (QEMSCAN).

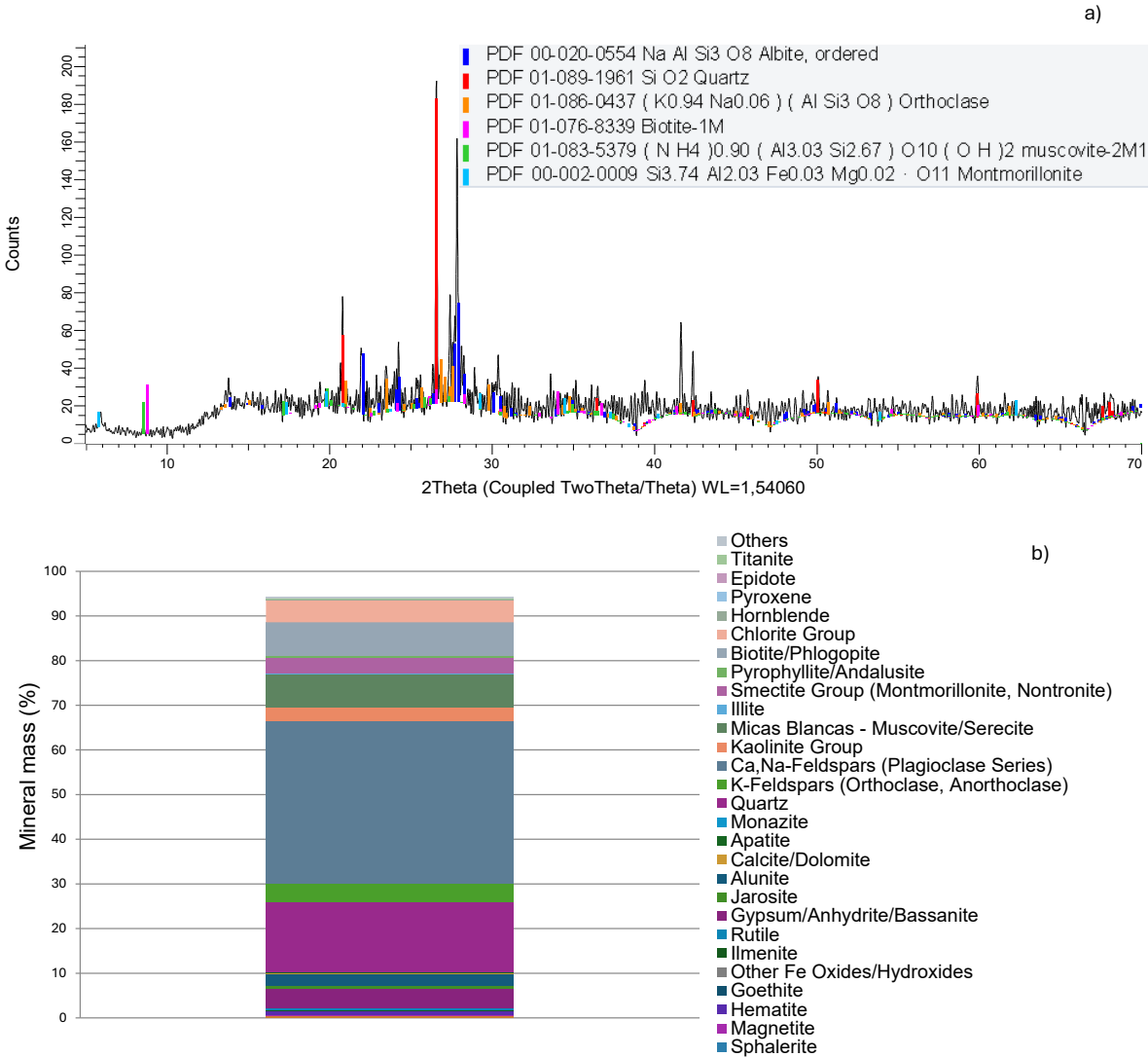


Fig. 2. Characterization of the MT by a) X-ray diffraction (XRD) and b) quantitative evaluation of minerals by scanning electron microscopy (QEMSCAN).

The specific surface area of MT was measured according Brunauer–Emmett–Teller isothermal analysis (BET) using a Nova 600 from Anton Paar (Austria) equipment obtaining a value of 122 m²/g, with an error of 2%.

The LL was sampled from the authorized landfill in Coquimbo called El Panul (29° 59' 56" S, 71° 23' 21" W, Chile), where the domestic solid wastes of Coquimbo, Chile, are disposed of. The main characteristics of LL are detailed in Table 1.

Table 1. Raw landfill leachate characteristics.

Parameter	Value	Standard deviations
TOC (mg/L)	4192.6	402
COD (mg/L)	8350.4	498.2
pH	8.9	0.3
Total solids (mg/L)	20,100	350
Total Iron (mg/L)	41.600	260
Abs ₂₅₄	0.4	0.03
Faecal coliforms (mpn)	0	0
Chloride (mg/L)	6230.4	550.3

mpn: most probable number

2.3.- Landfill Leachate Treatments

To improve the performance of the sonophotocatalytic process, which is negatively affected by the shadow effect, the leachate was pretreated by coagulation/flocculation with 1000 mg/L of FeCl₃, following the methodology of Poblete and Painemal, (2018). The mixture was stirred at 150 rpm, allowed to settle for 6 hours, and then filtered through a 5 µm filter.

To enhance the performance of the sonophotocatalytic process, which is negatively affected by the shadow effect, the LL was pre-treated using the coagulation/flocculation process to remove suspended solids. This pretreatment consisted of adding 1000 mg/L of coagulant to the LL, which was FeCl₃ (≥99% of purity, Merck), and stirring the mixture at 150 rpm, according to the methodology published by our research group (Poblete and Painemal, 2018). After that, the LL was left to stand for 6 hours to recover the supernatant, which was then submitted to a filtration process with a 5 µm-pore size filter.

The pretreated LL was placed in a sonophotoreactor, which is a cylindrical container with a volume of 1000 mL, and the LL was submerged in a probe from the US system (Sonic-generator VCX-500), which generates an ultrasonic wave of 20 kHz and 500 W of power. Additionally, the LL was submerged in a UVc lamp that emits at 254 nm, with 40 W of power (see Figure 3). In all the runs, to protect the US probe, the temperature of the sonophotoreactor was set to 20 °C using a cooling jacket, which was controlled using a chiller of 250 W. The solution was stirred using a magnetic stirrer set at 500 rpm.

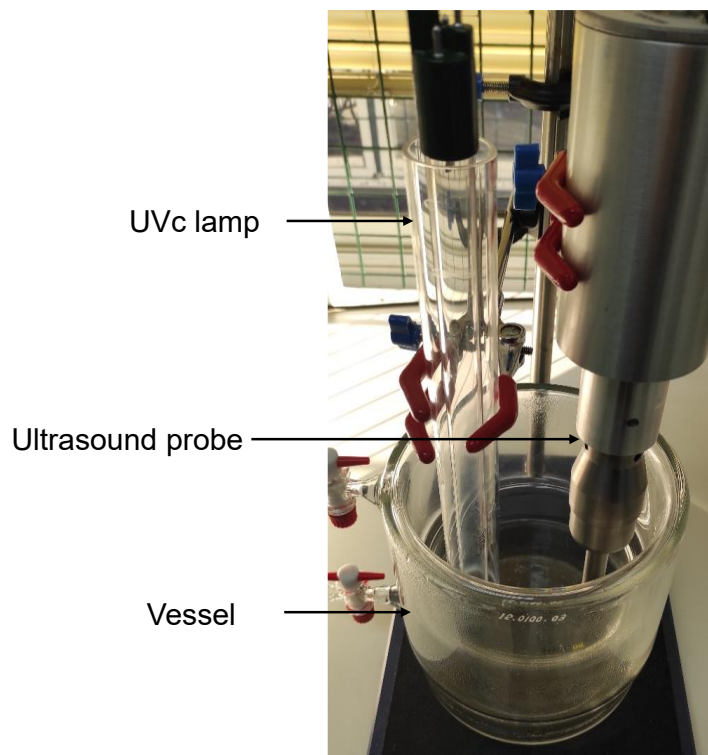


Fig. 3. Picture of the sonophotoreactor.

The ultrasonic experiments were conducted at 100% power capacity of the equipment, and the pulse and silent times were set to change continuously from 0 to 10,000 ms. The factorial design experiment lasted 60 min for each run, and all runs were performed in triplicate.

2.4.- Factorial Design

Taking into consideration that it is the first study focused on the use of MT as a catalyst in the US and photocatalytic process, it was necessary to establish the importance of factors, such as the catalyst load, the concentration of H_2O_2 and the pH of the solution, as well as to determine the range of these factors that maximise the removal of organic pollutants the LL.

Consequently, a two-level full factorial design with centre points was carried out, where the factors were: catalyst load (factor A, with levels of 200, 1000 and 2000 mg/L), concentration of H_2O_2 (factor B, with levels of 1000, 2000 and 3000 mg/L) and pH of the solution (factor C, with levels of 3, 6 and 8.9), as can be seen in Table 2. These levels were selected considering previous results using an industrial solid waste as a catalyst (Poblete et al., 2011; Poblete et al., 2024b). MT was added to the sonophotoreactor in its original form, i.e., as a powder.

Table 2. Factorial experimental design for sonophotocatalytic experiments

	[Catalyst] (level)	[H_2O_2] (level)	pH (level)
1	200 mg/L (-1)	1000 mg/L (-1)	8.9 (1)

2	200 mg/L (-1)	1000 mg/L (-1)	3	(-1)
3	200 mg/L (-1)	3000 mg/L (1)	8.9	(1)
4	2000 mg/L (1)	1000 mg/L (-1)	3	(-1)
5	2000 mg/L (1)	3000 mg/L (1)	8.9	(1)
6	2000 mg/L (1)	1000 mg/L (-1)	8.9	(1)
7	1000 mg/L (0)	2000 mg/L (0)	6	(0)
8	2000 mg/L (1)	3000 mg/L (1)	3	(-1)
9	200 mg/L (-1)	3000 mg/L (1)	3	(-1)

268

269 The response of the factorial design was evaluated according to the removal of TOC
270 and aromatic compounds (Abs₂₅₄). Data were analysed using the software program
271 Minitab 19.

272 The factorial design with runs of 60 min duration was carried out as a first approach
273 focused on the use of MT as a catalyst in the sonophotocatalytic process, and since
274 all experiments lasted the same amount of time, the results can be used to compare
275 the effect of the factors and to identify which comparison of levels optimizes the
276 outcome, in order to subsequently carry out a long-term experiment with the
277 optimized conditions. Therefore, the optimal factor levels for TOC and aromatic
278 compound removal were applied in a 3-hour experiment of a sonophotocatalytic
279 process, to evaluate the removal of pollutants from LL and the change in its
280 biodegradability throughout the treatment, using the Zahn-Wellens test, because
281 Zahn-Wellens bioassay is more proper for biodegradability evaluations over time (da
282 Costa et al., 2018) and is adequate to provide valuable information referred to the
283 biodegradability improvement and establish the optimal point to stop the chemical
284 process and combine to a biological treatment considering the environmental
285 requirements for discharge (Welter et al., 2018).

286 For all the runs, the MT used in the reactor was dried at 105 °C for two hours and
287 particle sizes selected were in the range of 75-150 µm (Poblete et al., 2011).

288

289 2.5.- Analytical Determination and Equipment

290 To measure the concentration of TOC in the LL, 50 µL of samples were injected into
291 a Shimadzu TOC-L (Japan), at 650 °C combustion, through acid-catalysed, using a
292 non-dispersive infrared (NDIR) detector. Shimadzu provided all devices and
293 reagents used for TOC measurements. The aromatic compounds (Abs₂₅₄) present
294 in LL were measured using a UV/VIS spectrophotometer at 254 nm (Liu et al., 2015)
295 (Optizen Pop Series UV/VIS, Mecasys, Korea). Chemical oxygen demand of LL was
296 determined through the colourimetric technique (EPA 410.4 protocol), using a
297 spectrophotometer Hanna HI83099 (Hanna Instruments, USA). Total copper
298 present in LL was established according to the Bicinchoninate Acid Method (HI-
299 93702-01). The Iron and aluminium (EPA phenanthroline 315B and HI93712-01
300 methods, respectively) with the Hanna HI83099 spectrophotometer.

The concentration of H₂O₂ in the solution was measured according to the iodometric method (at 350 nm) (Kormann et al., 1988), using the Hanna HI83099 spectrophotometer.

To evaluate the change in the biodegradability of the LL due to the sonophotocatalytic process, the Zahn-Wellens test was carried out, according to the OECD, Directive 88/303/EEC protocol (OECD, 1992).

The test lasts 28 days in an open vessel, where the evaluated water is adjusted to pH≈7, and the mixture is continuously stirred at 500 rpm and kept at room temperature. The biological solutions are constituted by previously centrifuged activated sludge that was obtained from an urban wastewater treatment plant located in Tongoy (lat 30°15'27"S, long 71°29'33"W), Coquimbo, and mineral nutrients (K₂HPO₄, KH₂PO₄, NH₄Cl, Na₂HPO₄, MgSO₄, CaCl₂, and FeCl₃).

The blank and control runs were carried out using distilled water and glucose, respectively. The biodegradation (%) was calculated according to the following equation:

$$D_t = 1 - \frac{(C_t - C_B)}{(C_A - C_{BA})} \quad (5)$$

where D_t is the percentage of biodegradation, C_t and C_B were the TOC of the mixture concentration (mg/L) in the mixture and in the blank, respectively, measured at a t time; C_a and C_{BA} were the TOC of the mixture and in the blank, respectively, measured 3 h after the beginning of the run. The treated LL is considered biodegradable when biodegradation is higher than 70%.

Also, an Inductively Coupled Plasma Mass Spectrometry (ICP-MS) Analysis of Water was carried out in the presence of the MT mass and at the pH conditions that improved the pollutant removal in the factorial design, under US irradiation. For this purpose, the water samples were filtered at 0.22 μm and analysed using a Thermo Fisher iCAP TQe ICP-MS-TQ in S-SQ-iKED mode. The detection limit of the measurement is 100 ng/L.

3. Results and Discussion

3.1.- Factorial design

Figure 4 shows the effect estimates of the degradation of pollutants due to the evaluated factors, where it is possible to observe that factor C (pH of the solution) is the most crucial parameter in the removal of TOC and aromatic compounds from the LL. This relevant impact on the oxidation process can be because of pH on the solubilization of iron and copper in the LL, which enhances the presence of this catalyst in photo-Fenton and photo-Fenton-like processes, respectively (Zong et al., 2025; Bhaskar et al., 2025).

The normal effects plot has irregular intervals on the Y-axis because it uses a scale based on the quantiles of the standard normal distribution. This representation

allows you to visually identify significant effects that deviate from the straight line expected under the null hypothesis.

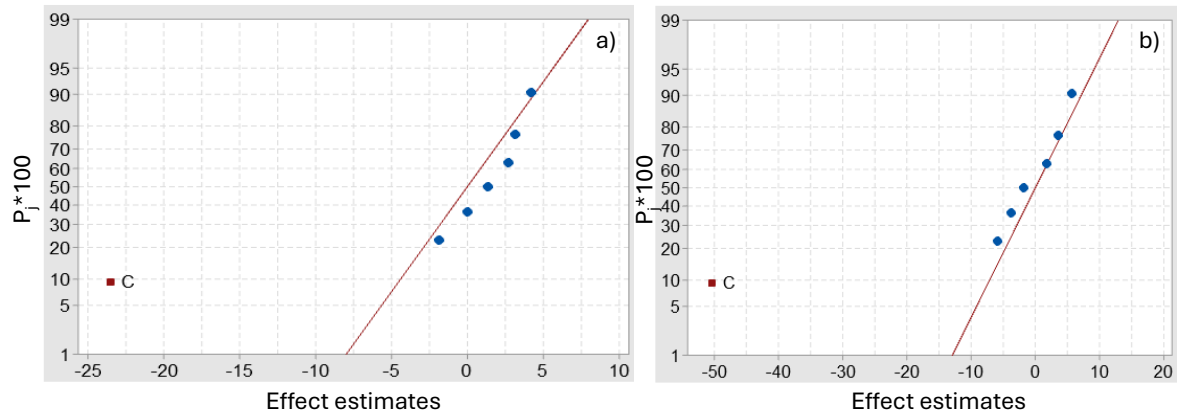


Figure 4. Probability versus effect estimates for a) TOC and b) Aromatic compounds removal (%).

The Pareto chart, depicted in Figure 5, presents the influence of the evaluated factor, where the results agree with those shown in Figure 4, where the pH is the most relevant factor on the effect of removal of TOC and aromatic compounds from the LL, showing a significant difference. The reason lies in the crucial impact of the solution pH on the sonophotocatalytic process (Kallawar et al., 2024).

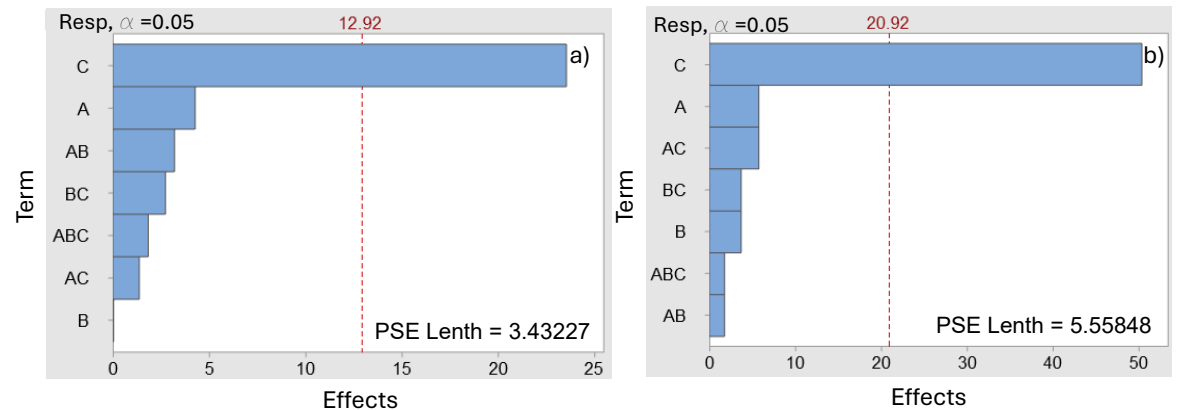


Figure 5. Pareto chart of effects for TOC and Aromatic compounds removal (%). Factors: A ([catalyst]), B (H_2O_2) and C (pH). α represents Statistical significance level and PSE length represents Pseudo Standard Error. p-value=0.05.

The levels of the factors that maximise the removal of TOC and aromatic compounds are a higher load of catalyst, a higher concentration of H_2O_2 and lower pH (see Fig. 6). Under the optimised conditions, it was possible to get a removal of 29.8 and 50.2% of TOC and aromatic compounds, respectively. Also, the removal was very low at lower load of catalyst, lower concentration of H_2O_2 , and higher pH (5 % for TOC and 2% for aromatic compounds). The results obtained in the optimized

condition are in agreement with those obtained in previous research of our investigation group, which achieved a removal of 50.2% of aromatic compounds using an industrial fly ash as catalyst, 576 kHz of US frequency and a solution of LL adjusted at pH to 3 (Poblete et al., 2024). Also, these results are lower than those obtained in a research that used 950 mg/L of TiO₂ as photocatalyst and a UVC lamp to depurate a LL, presenting a TOC removal of 72.8% and the difference can be due to the power of the UVC lamp, which was 400 W (Aibuedefe and Tina, 2024), much higher than that used in this research.

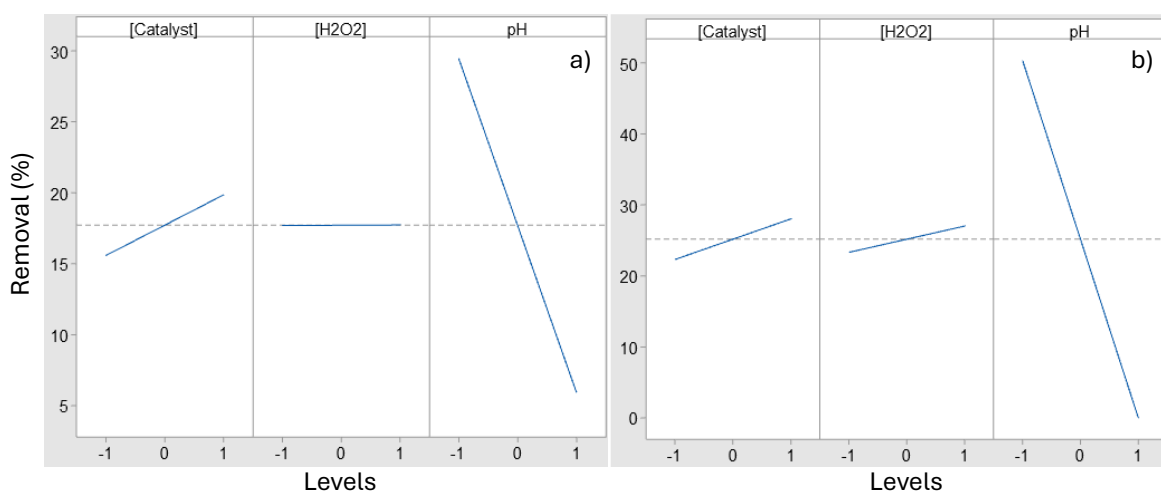


Figure 6. Mean a) TOC and b) Aromatic compounds removal (%).

The better results obtained using a higher load of MT can be explained by considering that a high load of catalyst enhances the area accessible for the adsorption process and the production of oxidant radicals, causing an improvement in the degradation (Srisangari and Marathe, 2024). Nevertheless, when the optimum catalyst load is exceeded, the solution becomes turbid, increasing the turbidity of water by reducing the efficiency of UV radiation in the aqueous medium (Gao et al., 2022).

Also, Figure 6 shows that the removal of aromatic compounds of the LL was enhanced when a higher concentration of H₂O₂ was added to the solution, and this can be because this reagent, in the presence of US cavitation, improves the production of hydroxyl radicals (Wang and Wang, 2020).

In addition, when exposed to UV-C irradiation, the photolysis of H₂O₂ is induced, producing more hydroxyl radicals, as illustrated in the following equation:



Therefore, a high concentration of H₂O₂, enhances the degradation of pollutants; however, when the presence of this reagent is higher than the optimal, a scavenger of HO[•] can be formed due to recombination, generating hydroxyperoxyl radical,

which have lower oxidant potential than hydroxyl radicals (Merdoud et al., 2024; Innocenzi et al., 2019).

Also, as can be seen in Figure 6, the removal of pollutants is higher when the level of the factor pH is lower, at pH=3. This is due to the low recombination of HO[•] under acidic conditions, enhancing the degradation of organic compounds (Thomas et al., 2020). Considering the effect of pH on the US process, the pollutants accumulate in the gas-liquid interface of the bubble being attacked for HO[•] in acid conditions (Ghosh and Sahu, 2024). It is necessary to consider that the oxidation of organic compounds happens in both the interfacial film and gaseous zone due to pyrolysis and the hydroxyl radicals at lower pH. Additionally, in acid conditions, there is an electrostatic attraction between the oppositely hydrophobic molecules and the gas-liquid interface, enhancing the degradation of pollutants (Pirsaheb and Moradi, 2020).

The use of the US process in photocatalytic treatment provokes local turbulence in the liquid, enhancing the mass transfer and increasing the availability of the reaction sites, while also promoting the dispersion of the MT particles, increasing their interaction with the pollutants (Ahmed and Mohamed, 2024). US cavitation generates high-frequency pressure waves that cause compression and expansion cycles, creating microjets with high pressure and temperature effects. This phenomenon destabilizes particles and promotes the dispersion of agglomerates due to intense shear forces, which increases the effective contact area between particles and improves process efficiency (Li et al., 2025)

As was described before, MT was mainly constituted of Feldspars (plagioclase Series), Quartz (SiO₂), Biotite/Phlogopite, Muscovite/Sericite, Cu-bearing Phyllosilicates, Montmorillonite, and TiO₂ rutile phase. Feldspars are crystalline with amorphous fractions of aluminosilicate and are considered adsorbent materials, where stability ensures that the sorptivity capacity is enhanced at elevated temperature (Youssef et al., 2021), including the plagioclase series (Aghabeyk et al., 2022). In the case of Biotite/Phlogopite, under UV irradiation, its substance with a narrower band gap energy can be excited, producing h⁺/e⁻ pairs, promoting several reactions of oxidation (Mohamed, 2024). Muscovite is a layered silicate mineral (Chen et al., 2022), considered an adsorbent material and a heterogeneous catalyst, which can be used in wastewater treatment (Aboussabek et al., 2024), similar to natural inorganic diatomite, in terms of its adsorbent properties (Bai et al., 2024b).

Cu-bearing Phyllosilicate is a clay with an interesting capacity for the adsorption of organic pollutants present in water (Mamine et al., 2024). This mineral is constituted by atoms of oxygen and silicon, as a silica layer, and by aluminium atoms (alumina or aluminium hydroxide layer), and can be applied in wastewater treatment as an adsorbent material (Sanavada et al., 2023). In the MT, montmorillonite was also found, which is a clay that presents interesting adsorption capacity with a high surface area (Naing et al., 2022), where rapidity was demonstrated for wastewater treatment (Cao et al., 2025). Besides, it was established that montmorillonite stimulates the formation of OH[•] due to its presence of Fe, and when hydrogen

peroxide is added to the solution, under ultrasonic waves or UV irradiation (Demirtas et al., 2025). TiO_2 is a semiconductor under UV irradiation, which has shown a high photocatalytic ability, presenting chemical stability and biodegradability (Talukdar et al., 2020).

3.2.- Long-term experiments

Figure 7 shows the variation in the concentration of COD, TOC and aromatic compounds of pretreated LL as a function of treatment time, subjected to a sonocatalytic process under the conditions that optimise pollutant removal: 2000 mg/L of catalyst (MT), 3000 mg/L of H_2O_2 , and a solution adjusted to pH 3. As the treatment time increases, a progressive reduction in all three parameters is observed, indicating a sustained degradation of organic pollutants over time. After 3 h of treatment, the removal of TOC, COD, and aromatic compounds were 84.9%, 69.6%, and 88.7%, respectively.

As can be seen, the results obtained in these runs are better than the obtained in the factorial design, that lasted 60 minutes each, where the higher removal of TOC was 29.8%, and is due to the longer duration of this experiment, 180 mins, allowing a highest oxidation of organic matter (Mukhtiar et al., 2025; Rostami et al., 2025).

These results are similar to those obtained using the sono-photo-Fenton process, in the treatment of a LL, achieving a removal of COD and aromatic compounds of 93% and 77%, respectively (Bellouk et al., 2023), using the traditional reagents of the photo-Fenton process, showing that these processes are very competitive in comparison with other AOPs, according to the phytotoxicity evaluation. These high results of the removal of pollutants can be due to the interaction of the different constituents of the MT, due to its photocatalytic and adsorbent properties.

Also, the results obtained in this research are higher than those reported in a study where the treatment of LL was evaluated using the commercial TiO_2 of Degussa as catalysis and, after 3 h. of irradiation with a UVC lamp, a TOC removal of 76% was achieved (Becerra et al., 2020). The difference between both processes may be attributed to the fact that, in the case of the present study, a sonophotocatalytic process was applied.

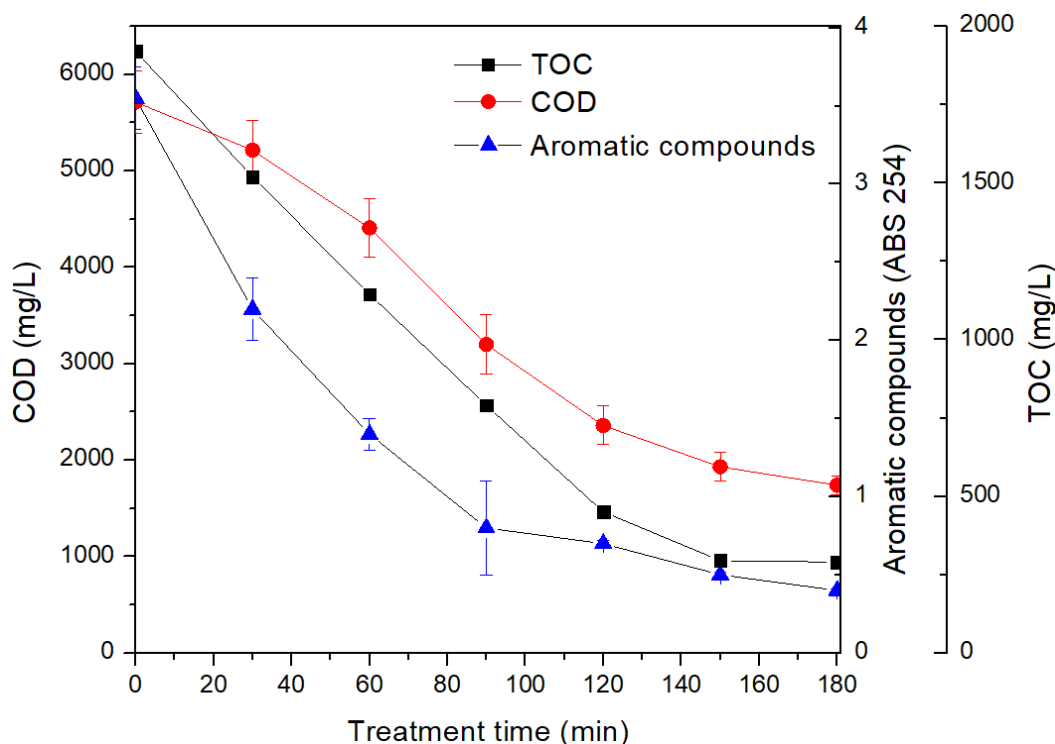


Figure 7. Change in the concentration of COD, TOC, and aromatic compounds of LL, submitted to a sonocatalytic process using 2000 mg/L of MT as catalyst, 3000 mg/L of H₂O₂, and solution at pH 3.

3.3.- Blank experiments

Considering MT's capacity as a photocatalytic and adsorbent material and the participation of the US process, to elucidate the effect of the involved processes in the removal of pollutants from LL, blank experiments were conducted for photocatalysis, ultrasound, and adsorption (in the dark), all three using 2000 mg/L MT, at pH=3, for 3 h of run. In the case of the adsorption process, it was conducted separately in the dark, without UV irradiation and without ultrasound.

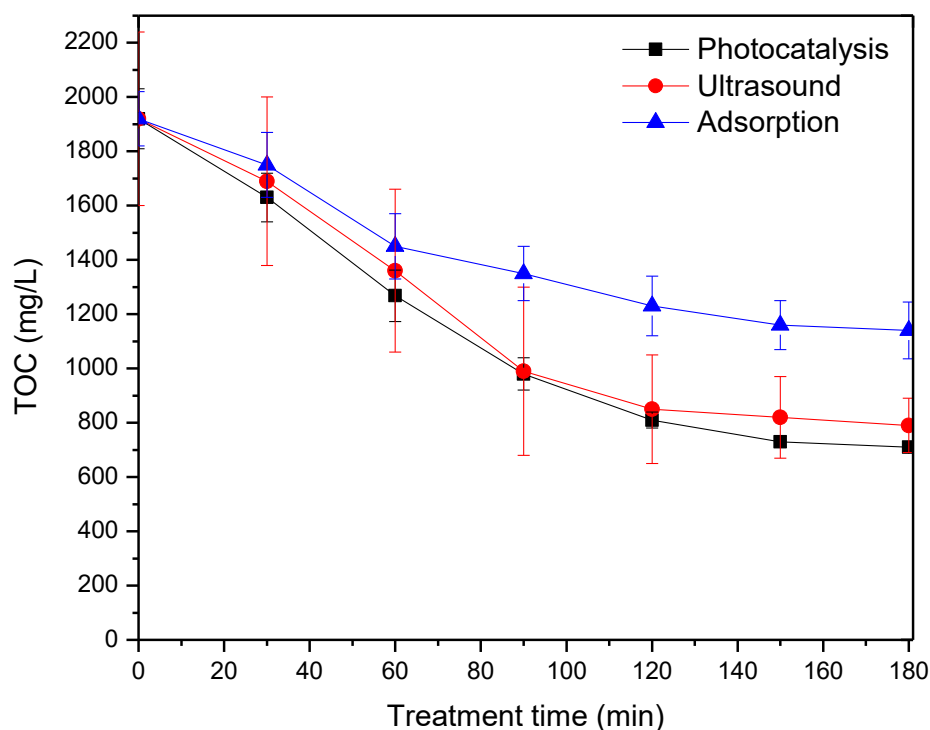


Figure 8. Change in the concentration of TOC of LL, submitted to photocatalysis, ultrasound and adsorption (dark) process, using 2000 mg/L of MT as catalyst, 3000 mg/L of H_2O_2 and solution at pH 3.

Figure 8 shows that the photocatalytic process, using MT as a catalyst, offers the highest removal of pollutants, followed by the US process, while the lowest performance was obtained by the adsorption process, with TOC removals of 63.1%, 58.9%, and 40.6%, respectively. These results show that the main process that has an effect on oxidation was the photocatalytic process, possibly due to the presence and interaction of Biotite/Phlogopite, montmorillonite and TiO_2 , which under UV irradiation and H_2O_2 can produce a significant amount of hydroxyl radicals, triggering a series of oxidation reactions (Mohamed, 2024; Aboussabek et al., 2024; Demirtas et al., 2025; Talukdar et al., 2020).

3.4.- Assessment of biodegradability

As can be observed in the results obtained in this research, a high removal of the evaluated organic pollutant in treating LL using MT was achieved. However, it can be inferred that using solid mining waste can be dangerous or complex, considering the presence of heavy metals that can be leached in solution (Bai et al., 2022), that can be leached under acid conditions (Bai et al., 2024a) and interact with the constituents of the matrix. Therefore, the change of concentration of iron, copper, and aluminium was measured before and after the sonophotocatalytic process, using 2000 mg/L MT, at pH=3, for 3 h of run. No increase was observed in the concentration of iron, copper, and aluminium in the LL submitted to this process.

The results of the biodegradability assay carried out on the LL submitted to the pretreatment (coagulation/flocculation process) and on the LL submitted to sonophotocatalysis (also pretreated) are depicted in Fig. 9. The control (distilled water and glucose) and the LL submitted to a sonophotocatalysed treatment. The LL had an initial concentration of 705.3 mg/L of TOC, and after the bioassay present a TOC degradation higher than 70%, validating the test. Also, it can be seen that the oxidation processes achieved greater TOC removal than the control, obtaining 83.2% and 75.0%, respectively. In the case of the raw LL and the submitted to the pretreatment, the removal of TOC was 7.2 and 45.9%, respectively, after 28 days of assay. The very low biodegradability of the raw LL obtained is consistent with the results obtained (de Pauli et al., 2018), who obtained a biodegradability of the raw LL of 10%.

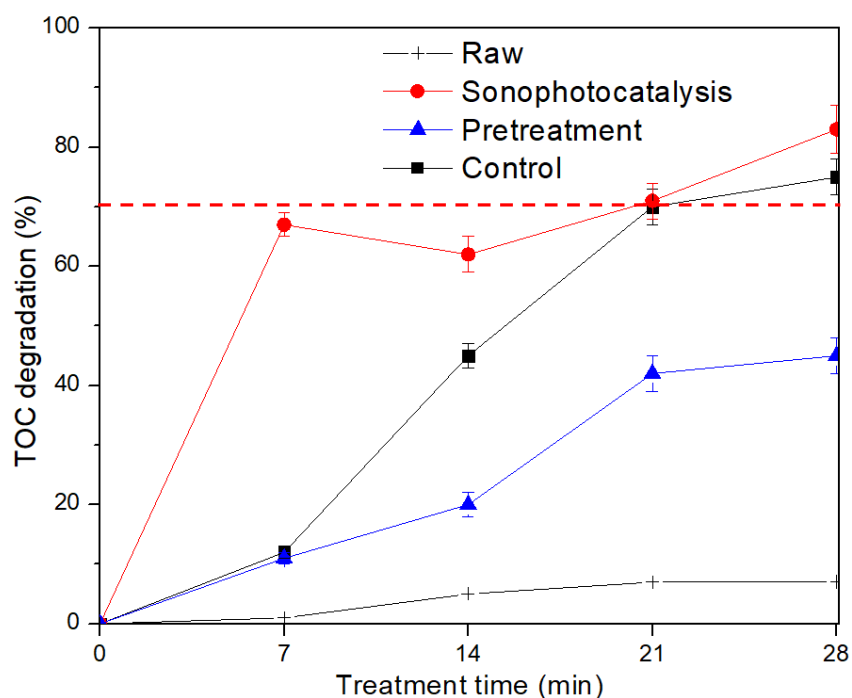


Figure 9. Biodegradability by Zahn-Wellen assay for control, pre-treated LL and sonophotocatalyzed LL.

After 28 days of bioassay, these results can be attributed to the transformation of organic substances into sub-products with lower toxic substances (de Pauli et al., 2018) such as fulvic acids present in the LL (Gomes et al., 2021) chlorinated aliphatic compounds, surfactants, organic dyes and aromatic compounds into less complex forms, which increases the biodegradability and reduces their toxicity (Gałwa-Widera, 2025).

In Figure 9, the results of the Inductively Coupled Plasma Mass Spectrometry (ICP-MS) Analysis of water at pH 3 and in the presence of 2 mg/L of MT are presented.

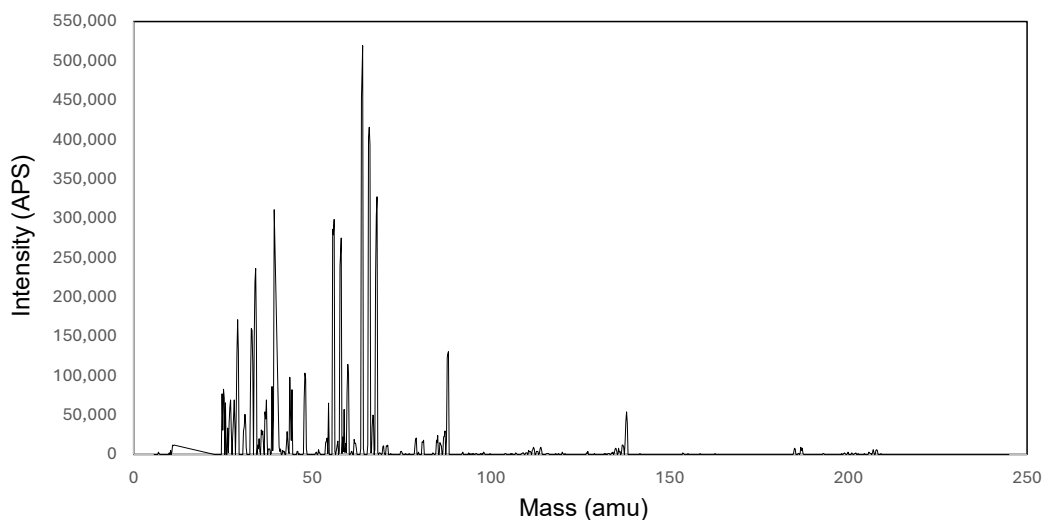


Figure 10. Inductively Coupled Plasma Mass Spectrometry Analysis of Water in the Presence of MT

The results show the presence of Ti, Si, Cu, Fe, K, Al, Li and Cl. However, as can be seen in the biodegradability analysis, these concentrations are not hazardous to the leachate.

3.5.- Circular Economy aspects

This research demonstrates the efficiency of using MT as catalysts in the treatment of LL. Additionally, it contributes to the circular economy approach, as it enables the revaluation of mining waste that has historically been considered an environmental liability. From a circularity perspective, the MT used experimentally can be used directly as a functional raw material in a wastewater treatment process. Considering a load of 2000 mg/L of MT to treat leachate, which has very high volumes in a landfill, and in the case of El Panul, where the LL studied was sampled, has a total volume of 280 m³, the process would require a quantity of 560 tons of MT. Although no life cycle assessment was conducted, the direct reuse of MT, without requiring intensive energy for structural modification, constitutes an advance in the design of environmentally sustainable processes. In addition, it was verified that there is no leaching of heavy metals (Fe, Cu, Al) during the process, providing key evidence on the environmental safety of the circular use of hazardous waste.

Another relevant study focused in the used of waste as precursor of catalyst was published by Yang et al., (2025) who evaluated the performance of a material, prepared with Fe-Ni monometallic and bimetallic catalysts, from rice husks, showing a high synergy between Fe and Ni and reduced the possibility of active site deactivation.

4.- Conclusions

This study demonstrates the feasibility of reusing MT as a heterogeneous catalyst in the sonophotocatalytic treatment of mature landfill leachate. The MT, primarily composed of feldspars, phyllosilicates, montmorillonite, and rutile TiO_2 , exhibited both photocatalytic and adsorptive properties that contributed to the effective degradation of organic pollutants.

A full factorial design identified pH as the most influential parameter, with the highest removal efficiencies observed at acidic conditions (pH 3), high catalyst loading (2000 mg/L), and elevated hydrogen peroxide concentration (3000 mg/L). Under optimized conditions, TOC, COD, and aromatic compounds were removed by 84.9%, 69.6%, and 88.7%, respectively, within 3 hours of treatment.

The sonophotocatalytic process also significantly enhanced the biodegradability of LL, as evidenced by the Zahn-Wellens test, with post-treatment values exceeding the 70% threshold for biodegradability. Importantly, no leaching of potentially toxic metals (Fe, Cu, Al) from the MT was observed under the applied conditions, supporting the environmental safety of this approach.

These findings provide a novel alternative for the valorisation of MT, contributing to circular economy strategies in the mining and waste management sectors. Future research should focus on long-term stability, catalyst reusability, and the scale-up of the treatment process to validate its applicability at an industrial level.

Acknowledgments

The authors thank to Fondecyt N° 1210841 for the financial support, and MAINI® in the for convenio Cia. Minera Cerro Colorado-UCN 2007-2013 and DRX-FIC Regional 2008 EQU 25 Conicyt 2009-2010.

References

302 B OECD GUIDE LINE FOR TESTIN G OF CHEMICALS, 92AD.

Aboussabek, A., Boukarma, L., El Qdhy, S., Ousaa, A., Zerbet, M., Chiban, M., 2024. Experimental investigation, kinetics and statistical modeling of methylene blue removal onto Clay@Fe₃O₄: Batch, fixed bed column adsorption and photo-Fenton degradation studies. *Case Stud Chem Environ Eng* 9, 100580. <https://doi.org/10.1016/J.CSCEE.2023.100580>

Aghabeyk, F., Azadmehr, A., Hezarkhani, A., 2022. Fabrication of feldspar-based geopolymers from perlite toward decontamination of heavy metals from aqueous solution: Hydrolysis process, characterizations, kinetic and isotherm studies. *J Environ Chem Eng* 10, 108087. <https://doi.org/10.1016/J.JECE.2022.108087>

Ahmed, M.A., Mohamed, A.A., 2024. Advances in ultrasound-assisted synthesis of photocatalysts and sonophotocatalytic processes: A review. *iScience* 27, 108583. <https://doi.org/10.1016/J.ISCI.2023.108583>

604 Aibuedefe, A.F., Tina, A.E., 2024. Optimization of landfill leachate through hybrid
605 treatment of phytoremediation and photocatalysis using response surface
606 methodology. *Sustain Chem Environ* 5.
607 <https://doi.org/10.1016/j.scenv.2024.100076>

608 Alanís, F., Nordenflycht, R., Guerrero, M., Villalobos, K., Poblete, R., Rodríguez,
609 C.A., Pérez, N., Cortés, E., Torres-Palma, R.A., 2025. Sonoluminescence and
610 H₂O₂ produced in water under different ultrasound operating conditions
611 applied to the sono-photo-Fenton landfill leachate treatment. *Chem Eng*
612 *Process: Process Intensif* 110246. <https://doi.org/10.1016/J.CEP.2025.110246>

613 Almeida-Naranjo, C.E., Guerrero, V.H., Villamar-Ayala, C.A., 2023. Emerging
614 Contaminants and Their Removal from Aqueous Media Using
615 Conventional/Non-Conventional Adsorbents: A Glance at the Relationship
616 between Materials, Processes, and Technologies. *Water (Switzerland)*.
617 <https://doi.org/10.3390/w15081626>

618 Arvaniti, O.S., Ioannidi, A., Politi, A., Miserli, K., Konstantinou, I., Mantzavinos, D.,
619 Frontistis, Z., 2022. Dexamethasone degradation in aqueous medium by a
620 thermally activated persulfate system: Kinetics and transformation products. *J.*
621 *Water Process Eng.* 49, 103134. <https://doi.org/10.1016/J.JWPE.2022.103134>

622 Bai, B., Bai, F., Li, X., Nie, Q., Jia, X., Wu, H., 2022. The remediation efficiency of
623 heavy metal pollutants in water by industrial red mud particle waste. *Environ*
624 *Technol Innov* 28, 102944. <https://doi.org/10.1016/J.ETI.2022.102944>

625 Bai, B., Chen, J., Bai, F., Nie, Q., Jia, X., 2024a. Corrosion effect of acid/alkali on
626 cementitious red mud-fly ash materials containing heavy metal residues.
627 *Environ Technol Innov* 33, 103485. <https://doi.org/10.1016/J.ETI.2023.103485>

628 Bai, B., Zhang, B., Chen, J., Feng, H., 2024b. Development of a natural inorganic
629 diatomite curing agent on heavy metal-contaminated loess. *Phys. Chem.*
630 *Earth, Parts A/B/C* 136, 103790. <https://doi.org/10.1016/J.PCE.2024.103790>

631 Becerra, D., Soto, J., Villamizar, S., Machuca-Martínez, F., Ramírez, L., 2020.
632 Alternative for the Treatment of Leachates Generated in a Landfill of Norte de
633 Santander–Colombia, by Means of the Coupling of a Photocatalytic and
634 Biological Aerobic Process. *Top Catal* 63, 1336–1349.
635 <https://doi.org/10.1007/s11244-020-01284-1>

636 Bellouk, H., Danouche, M., El Mrabet, I., Tanji, K., Khalil, F., Nawdali, M., El
637 Ghachtouli, N., Zaitan, H., 2023. Remediation of the landfill leachate of Fez
638 city (Morocco) by sono-photo-Fenton process: Cost and phytotoxicity
639 assessment. *J Water Process Eng* 56, 104565.
640 <https://doi.org/10.1016/J.JWPE.2023.104565>

641 Bhaskar, S., Apoorva, K. V., Ashraf, S., Athul Devan, T., 2025. Synthesis and
 642 application of iron nanoparticles from scrap metal for triclosan degradation in
 643 water via Fenton and Sono-Fenton oxidation. *Waste Manag Bull* 3, 293–300.
 644 <https://doi.org/10.1016/J.WMB.2025.01.012>

645 Botero, Y.L., Cisternas, L.A., Demers, I., Benzaazoua, M., 2024. Insights into the
 646 design of polymetallic ore flotation circuits, including tailing desulfurization.
 647 *Miner Eng* 205, 108475. <https://doi.org/10.1016/J.MINENG.2023.108475>

648 Campos-Medina, F., Ojeda-Pereira, I., Guzmán, J., Aspillaga, V.R., Ferreira, J.S.,
 649 2023. What do we investigate when we research on mine tailings in Chile? An
 650 interpretative approach. *Extr Ind Soc*
 651 <https://doi.org/10.1016/j.exis.2023.101318>

652 Cao, C., Huo, T., Liu, P., Long, J., Ma, Y., Jahan, S.I., Manjoro, T.T., Dong, F., 2025.
 653 Montmorillonite-sodium alginate/chitosan beads: A green potential solution for
 654 phosphorus removal from wastewater and slow-release phosphorus fertilizer
 655 application. *Int J Biol Macromol* 305, 141276.
 656 <https://doi.org/10.1016/J.IJBIOMAC.2025.141276>

657 Chen, X., Liu, E., Zhang, D., Zhang, Z., Dong, Q., Zhang, X., Ding, X., Chen, S.,
 658 Zhu, X., 2022. Synthesis of novel muscovite loaded nano Ag/Cu₂-xFe_xO
 659 composites with excellent visible-light responsive photocatalysis. *Opt Mater*
 660 (Amst) 124, 112002. <https://doi.org/10.1016/J.OPTMAT.2022.112002>

661 da Costa, F.M., Daflon, S.D.A., Bila, D.M., da Fonseca, F.V., Campos, J.C., 2018.
 662 Evaluation of the biodegradability and toxicity of landfill leachates after
 663 pretreatment using advanced oxidative processes. *Waste Manag* 76, 606–613.
 664 <https://doi.org/10.1016/J.WASMAN.2018.02.030>

665 de Pauli, A.R., Espinoza-Quiñones, F.R., Trigueros, D.E.G., Módenes, A.N., de
 666 Souza, A.R.C., Borba, F.H., Kroumov, A.D., 2018. Integrated two-phase
 667 purification procedure for abatement of pollutants from sanitary landfill
 668 leachates. *CHEM ENG J* 334, 19–29.
 669 <https://doi.org/10.1016/J.CEJ.2017.10.028>

670 Demirtas, E.A., Açikel, Y.S., Aşçı, Y., 2025. A full factorial design for the
 671 decolorization of real textile wastewater using iron-rich montmorillonite by
 672 sonocatalytic process. *Chem Eng Process: Process Intensif* 208, 110111.
 673 <https://doi.org/10.1016/J.CEP.2024.110111>

674 Gałwa-Widera, M., 2025. The influence of the ultrasonic field on the efficiency of
 675 leachate treatment in the SBR reactor. *Desalination Water Treat* 321, 101025.
 676 <https://doi.org/10.1016/J.DWT.2025.101025>

677 Gao, Y., Yang, B., Yang, Y., Ming, H., Liu, G., Zhang, J., Hou, Y., 2022. Carbon-
 678 coated ZnFe₂O₄ nanoparticles as an efficient, robust and recyclable catalyst

679 for photocatalytic ozonation of organic pollutants. *J Environ Chem Eng* 10,
680 107419. <https://doi.org/10.1016/J.JECE.2022.107419>

681 Gareev, B.M., Abdrakhmanov, A.M., Sharipov, G.L., 2023. Single-bubble
682 sonoluminescence of aqueous suspensions of ZnS or Tb(acac)₃·H₂O
683 nanoparticles. *J Lumin* 260, 119863.
684 <https://doi.org/10.1016/J.JLUMIN.2023.119863>

685 Ghosh, S., Sahu, M., 2024. Ultrasound for the degradation of endocrine disrupting
686 compounds in aqueous solution: A review on mechanisms, influence of
687 operating parameters and cost estimation. *Chemosphere* 349, 140864.
688 <https://doi.org/10.1016/J.CHEMOSPHERE.2023.140864>

689 Gomes, A.I., Souza-Chaves, B.M., Park, M., Silva, T.F.C.V., Boaventura, R.A.R.,
690 Vilar, V.J.P., 2021. How does the pre-treatment of landfill leachate impact the
691 performance of O₃ and O₃/UVC processes? *Chemosphere* 278, 130389.
692 <https://doi.org/10.1016/J.CHEMOSPHERE.2021.130389>

693 Hiller, R., Weninger, K., Putterman, S.J., Barber, B.P., 1994. Effect of noble gas
694 doping in single-bubble sonoluminescence. *Science* (1979).
695 <https://doi.org/10.1126/science.266.5183.248>

696 Innocenzi, V., Prisciandaro, M., Centofanti, M., Vegliò, F., 2019. Comparison of
697 performances of hydrodynamic cavitation in combined treatments based on
698 hybrid induced advanced Fenton process for degradation of azo-dyes. *J*
699 *Environ Chem Eng* 7, 103171. <https://doi.org/10.1016/J.JECE.2019.103171>

700 Jagaba, A.H., Kutty, S.R.M., Lawal, I.M., Abubakar, S., Hassan, I., Zubairu, I.,
701 Umaru, I., Abdurrasheed, A.S., Adam, A.A., Ghaleb, A.A.S., Almahbashi,
702 N.M.Y., Al-dhawi, B.N.S., Noor, A., 2021. Sequencing batch reactor technology
703 for landfill leachate treatment: A state-of-the-art review. *J Environ Manag* 282,
704 111946. <https://doi.org/10.1016/J.JENVMAN.2021.111946>

705 Jari, Y., Najid, N., Necibi, M.C., Gourich, B., Vial, C., Elhalil, A., Kaur, P., Mohdeb,
706 I., Park, Y., Hwang, Y., Garcia, A.R., Roche, N., El Midaoui, A., 2025. A
707 comprehensive review on TiO₂-based heterogeneous photocatalytic
708 technologies for emerging pollutants removal from water and wastewater:
709 From engineering aspects to modeling approaches. *J Environ Manag* 373,
710 123703. <https://doi.org/10.1016/J.JENVMAN.2024.123703>

711 Joshi, S.M., Gogate, P.R., 2019. Treatment of landfill leachate using different
712 configurations of ultrasonic reactors combined with advanced oxidation
713 processes. *Sep Purif Technol* 211, 10–18.
714 <https://doi.org/10.1016/j.seppur.2018.09.060>

715 Kallawar, G., Thakare, N., Bonde, S., Barai, D., Bhanvase, B.A., Sonawane, A.,
716 Sonawane, S.H., Manickam, S., 2024. Exploring sonochemical synthesis for

717 photocatalyst nanocomposites in water and wastewater treatment: An in-depth
 718 review. *J Clean Prod* 485, 144279.
 719 <https://doi.org/10.1016/J.JCLEPRO.2024.144279>

720 Keyikoglu, R., Karatas, O., Rezaia, H., Kobya, M., Vatanpour, V., Khataee, A.,
 721 2021. A review on treatment of membrane concentrates generated from landfill
 722 leachate treatment processes. *Sep Purif Technol* 259, 118182.
 723 <https://doi.org/10.1016/J.SEPPUR.2020.118182>

724 Kirilova, M., Todorova, Y., Marinova, P., Bogdanov, T., Yotinov, I., Schneider, I.,
 725 Dinova, N., Topalova, Y., Benova, E., 2025. Plasma-assisted reduction of
 726 toxicity of landfill leachate, spiked with PFOA. *J Water Process Eng* 76,
 727 108190. <https://doi.org/10.1016/J.JWPE.2025.108190>

728 Kormann, C., Bahnemann, D.W., Hoffmann, M.R., 1988. Photocatalytic production
 729 of hydrogen peroxides and organic peroxides in aqueous suspensions of
 730 titanium dioxide, zinc oxide, and desert sand. *Environ Sci Technol*.
 731 <https://doi.org/10.1021/es00172a009>

732 Kösem, E., Ersöz, Ö.N., Yılmaz, R.N., Babaoğlu, D., Yazici Guvenc, S., Can-
 733 Güven, E., Varank, G., 2024. Sequential electrocoagulation and Fenton/Photo-
 734 Fenton processes for the treatment of membrane bioreactor effluent of landfill
 735 leachate. *Colloids Surf A Physicochem Eng Asp* 689, 133740.
 736 <https://doi.org/10.1016/J.COLSURFA.2024.133740>

737 Kwarciak-Kozłowska, A., Fijałkowski, K.L., 2021. Efficiency assessment of
 738 municipal landfill leachate treatment during advanced oxidation process (AOP)
 739 with biochar adsorption (BC). *J Environ Manag* 287, 112309.
 740 <https://doi.org/10.1016/J.JENVMAN.2021.112309>

741 Lei, Y., Hou, J., Fang, C., Tian, Y., Naidu, R., Zhang, J., Zhang, X., Zeng, Z.,
 742 Cheng, Z., He, J., Tian, D., Deng, S., Shen, F., 2023. Ultrasound-based
 743 advanced oxidation processes for landfill leachate treatment: Energy
 744 consumption, influences, mechanisms and perspectives. *Ecotoxicol Environ*
 745 *Saf* 263, 115366. <https://doi.org/10.1016/J.ECOENV.2023.115366>

746 Leiva G., M.A., Morales, S., 2013. Environmental assessment of mercury pollution
 747 in urban tailings from gold mining. *Ecotoxicol Environ Saf* 90, 167–173.
 748 <https://doi.org/10.1016/j.ecoenv.2012.12.026>

749 Li, X., Xu, Y., Li, N., Yang, B., Xia, H., Yu, K., Yang, H., Zhang, L., 2025.
 750 Ultrasound-assisted activation of zinc powder by antimony salts for the
 751 removal of Co and Cd from zinc sulfate solution. *Sep Purif Technol* 375,
 752 133781. <https://doi.org/10.1016/J.SEPPUR.2025.133781>

753 Lima, A.T., Kirkelund, G.M., Ntuli, F., Ottosen, L.M., 2022. Screening dilute sources
754 of rare earth elements for their circular recovery. *J Geochem Explor* 238,
755 107000. <https://doi.org/10.1016/J.GEXPLO.2022.107000>

756 Liu, Z.P., Wu, W.H., Shi, P., Guo, J.S., Cheng, J., 2015. Characterization of
757 dissolved organic matter in landfill leachate during the combined treatment
758 process of air stripping, Fenton, SBR and coagulation. *Waste Manag* 41, 111–
759 118. <https://doi.org/10.1016/J.WASMAN.2015.03.044>

760 Luo, X.S., Yu, S., Zhu, Y.G., Li, X.D., 2012. Trace metal contamination in urban
761 soils of China. *Sci Total Environ* 421–422, 17–30.
762 <https://doi.org/10.1016/J.SCITOTENV.2011.04.020>

763 Malafeevskiy, N., Lode, S., Røstad, J., Larsen, R.B., Aasly, K., 2025. An initial
764 characterization for revalorization of the Joma mine tailings, Norway. *Miner*
765 *Eng* 228, 109360. <https://doi.org/10.1016/J.MINENG.2025.109360>

766 Mamine, H., Boukachabia, M., Bendjeffal, H., Aloui, A., Metidji, T., Djebli, A.,
767 Bouhedja, Y., 2024. Removal of an organophosphate insecticide from aqueous
768 media using phyllosilicate clay: multivariable optimization, nonlinear kinetic
769 modelling and thermodynamic study. *Phosphorus Sulfur Silicon Relat Elem*
770 199, 536–549. <https://doi.org/10.1080/10426507.2024.2396443>

771 Mao, S., Zhao, Q., Ma, S., Du, Y., Shi, J., Zou, J., Qiu, Z., Yu, C., 2024. Heavy
772 metal pollution pressure in gold mines shows overall suppressed biochemical
773 sulfur cycle. *Int Biodeterior Biodegradation* 191.
774 <https://doi.org/10.1016/j.ibiod.2024.105807>

775 Marín, O.A., Ordóñez, J.I., Gálvez, E.D., Cisternas, L.A., 2020. Pourbaix diagrams
776 for copper ores processing with seawater. *Physicochem Probl Miner Process*
777 56, 625–640. <https://doi.org/10.37190/PPMP/123407>

778 Merdoud, R., Aoudjit, F., Mouni, L., Ranade, V. V., 2024. Degradation of methyl
779 orange using hydrodynamic Cavitation, H₂O₂, and photo-catalysis with TiO₂-
780 Coated glass Fibers: Key operating parameters and synergistic effects.
781 *Ultrason Sonochem* 103, 106772.
782 <https://doi.org/10.1016/J.ULTSONCH.2024.106772>

783 Min, M., Pu, H.F., He, X., Deng, S.Y., 2024. Anti-seepage performance and oxygen
784 barrier performance of the three-layered landfill cover system comprising
785 neutralized slag under extreme climate conditions. *Eng Geol* 342, 107750.
786 <https://doi.org/10.1016/J.ENGGEOL.2024.107750>

787 Mohamed, H.H., 2024. Natural pozzolana as standalone photocatalyst for water
788 treatment. *Inorg Chem Commun* 160, 111981.
789 <https://doi.org/10.1016/J.INOCHE.2023.111981>

790 Mohammad, A., Singh, D.N., Podlasek, A., Osinski, P., Koda, E., 2022. Leachate
 791 characteristics: Potential indicators for monitoring various phases of municipal
 792 solid waste decomposition in a bioreactor landfill. *J Environ Manag* 309,
 793 114683. <https://doi.org/10.1016/J.JENVMAN.2022.114683>

794 Moya, P.M., Arce, G.J., Leiva, C., Vega, A.S., Gutiérrez, S., Adaros, H., Muñoz, L.,
 795 Pastén, P.A., Cortés, S., 2019. An integrated study of health, environmental
 796 and socioeconomic indicators in a mining-impacted community exposed to
 797 metal enrichment. *Environ Geochem Health* 41, 2505–2519.
 798 <https://doi.org/10.1007/s10653-019-00308-4>

799 Mukhtiar, S., Rauf, S., Ibrahim, M.M., Ullah, H., Shehzad, F.K., Nadeem, M., Asif,
 800 H.M., Hussain, S., Saleem, U., 2025. Harnessing encapsulated
 801 polyoxometalate in MOFs for sonophotocatalytic Cr(VI) reduction: Unveiling
 802 the pathway to eco-friendly chromium remediation. *J Photochem Photobiol A*
 803 *Chem* 468, 116506. <https://doi.org/10.1016/J.JPHOTOCHEM.2025.116506>

804 Naing, H.H., Li, Y., Ghasemi, J.B., Wang, J., Zhang, G., 2022. Enhanced visible-
 805 light-driven photocatalysis of in-situ reduced of bismuth on BiOCl nanosheets
 806 and montmorillonite loading: Synergistic effect and mechanism insight.
 807 *Chemosphere* 304. <https://doi.org/10.1016/j.chemosphere.2022.135354>

808 Naveen, B.P., Mahapatra, D.M., Sitharam, T.G., Sivapullaiah, P. V., Ramachandra,
 809 T. V., 2017. Physico-chemical and biological characterization of urban
 810 municipal landfill leachate. *Environmental Pollution* 220, 1–12.
 811 <https://doi.org/10.1016/J.ENVPOL.2016.09.002>

812 Nesterov, D., Barrera-Martínez, I., Martínez-Sánchez, C., Sandoval-González, A.,
 813 Bustos, E., 2024. Approaching the circular economy: Biological,
 814 physicochemical, and electrochemical methods to valorize agro-industrial
 815 residues, wastewater, and industrial wastes. *J Environ Chem Eng* 12, 113335.
 816 <https://doi.org/10.1016/J.JECE.2024.113335>

817 Ni, Z., Ma, J., Nazarov, A.A., Yuan, Z., Wang, X., Ao, S., Ji, H., Guo, P., Qin, J.,
 818 2025. Improving the weldability and mechanical property of ultrasonic spot
 819 welding of Cu sheets through a surface gradient structure. *J Mater Res*
 820 *Technol* 36, 2652–2668. <https://doi.org/10.1016/J.JMRT.2025.03.301>

821 Pirsaeheb, M., Moradi, N., 2020. Sonochemical degradation of pesticides in
 822 aqueous solution: Investigation on the influence of operating parameters and
 823 degradation pathway-a systematic review. *RSC Adv* 10, 7396–7423.
 824 <https://doi.org/10.1039/c9ra11025a>

825 Poblete, R., Alanís, F., Serna-Galvis, E.A., Torres-Palma, R.A., 2024a. Depuration
 826 of landfill leachates using fly ash as a catalyst in solar advanced oxidation
 827 processes and a compost bioreactor. *J Environ Chem Eng* 12, 111651.
 828 <https://doi.org/10.1016/j.jece.2023.111651>

829 Poblete, R., Cortes, E., Pérez, N., Rodríguez, C.A., Luna-Galiano, Y., 2024b.
830 Treatment of landfill leachate by combined use of ultrasound and
831 photocatalytic process using fly ash as catalyst. *J Environ Manag* 349.
832 <https://doi.org/10.1016/j.jenvman.2023.119552>

833 Poblete, R., Otal, E., Vilches, L.F., Vale, J., Fernández-Pereira, C., 2011.
834 Photocatalytic degradation of humic acids and landfill leachate using a solid
835 industrial by-product containing TiO₂ and Fe. *Appl Catal B* 102, 172–179.
836 <https://doi.org/10.1016/j.apcatb.2010.11.039>

837 Poblete, R., Painemal, O., 2018. Solar Drying of Landfill-Leachate Sludge:
838 Differential Results Through the Use of Peripheral Technologies. *Environ Prog*
839 *Sustain Energy* 1–9. <https://doi.org/10.1002/ep.12951>

840 Rayaroth, M.P., Aravind, U.K., Aravindakumar, C.T., 2016. Degradation of
841 pharmaceuticals by ultrasound-based advanced oxidation process. *Environ*
842 *Chem Lett.* <https://doi.org/10.1007/s10311-016-0568-0>

843 Rostami, M., Badiei, A., Ziarani, G.M., Fasihi-Ramandi, M., Jourshabani, M., Lee,
844 B. –K, Rahimi-Nasrabadi, M., Ahmadi, F., 2025. C₃N₅-Cu-doped Co₃O₄
845 @NPC nano-cubes heterojunction architecture for sono-photocatalytic
846 degradation of the antibiotic sulfamethoxazole, electrocatalysis water splitting
847 for HER, and cytotoxic performance. *J Ind Eng Chem*
848 <https://doi.org/10.1016/J.JIEC.2025.04.031>

849 Rout, P.R., Zhang, T.C., Bhunia, P., Surampalli, R.Y., 2021. Treatment technologies
850 for emerging contaminants in wastewater treatment plants: A review. *Sci Total*
851 *Environ* 753, 141990. <https://doi.org/10.1016/J.SCITOTENV.2020.141990>

852 Sanavada, K., Shah, M., Gandhi, D., Unnarkat, A., Vaghasiya, P., 2023. A
853 systematic and comprehensive study of Eco-friendly bentonite clay application
854 in esterification and wastewater treatment. *Environ Nanotechnol Monit Manag*
855 20, 100784. <https://doi.org/10.1016/J.ENMM.2023.100784>

856 Seibert, D., Quesada, H., Bergamasco, R., Borba, F.H., Pellenz, L., 2019.
857 Presence of endocrine disrupting chemicals in sanitary landfill leachate, its
858 treatment and degradation by Fenton based processes: A review. *Process Saf*
859 *Environ* 131, 255–267. <https://doi.org/10.1016/J.PSEP.2019.09.022>

860 Seid-mohammadi, A., Asgari, G., Rafiee, M., Samadi, M.T., Nouri, F., Pirsaeheb, M.,
861 Asadi, F., 2021. Kinetic study of real landfill leachate treated by non-thermal
862 plasma (NTP) and granular sequential batch reactors (GSBR). *J Water*
863 *Process Eng* 43, 102245. <https://doi.org/10.1016/J.JWPE.2021.102245>

864 Sheik Moideen Thaha, S.K., Sathishkumar, P., 2025. Bisphenol A/Bisphenol F
865 mineralization in the presence of self-decorated carbon-
866 QDs@Bi₂O₂CO₃/Ti₃C₂/g-C₃N₄ nanocomposites under multi-frequency

867 ultrasound assisted sonophotocatalysis. Chem Eng J 505, 159578.
868 <https://doi.org/10.1016/J.CEJ.2025.159578>

869 Singa, P.K., Isa, M.H., Sivaprakash, B., Ho, Y.C., Lim, J.W., Rajamohan, N., 2023.
870 PAHs remediation from hazardous waste landfill leachate using fenton, photo
871 – fenton and electro - fenton oxidation processes – performance evaluation
872 under optimized conditions using RSM and ANN. Environ Res 231, 116191.
873 <https://doi.org/10.1016/J.ENVRES.2023.116191>

874 Srisangari, C., Marathe, K. V., 2024. Degradation of an emerging organic
875 contaminant via heterogeneous photocatalytic ozonation using V2O5 doped
876 ZnO under UV irradiation. J Water Process Eng 63, 105543.
877 <https://doi.org/10.1016/J.JWPE.2024.105543>

878 Su, H., Xie, Y., Cheng, X., Yang, Z., Mao, J., Yang, H., Xu, X., Pan, S., Hu, H.,
879 2024. The effect of dual-frequency ultrasound on synergistic Sonochemical
880 oxidation to degrade aflatoxin B1. Food Chem 457, 139708.
881 <https://doi.org/10.1016/J.FOODCHEM.2024.139708>

882 Talukdar, K., Jun, B.M., Yoon, Y., Kim, Y., Fayyaz, A., Park, C.M., 2020. Novel Z-
883 scheme Ag3PO4/Fe3O4-activated biochar photocatalyst with enhanced
884 visible-light catalytic performance toward degradation of bisphenol A. J Hazard
885 Mater 398, 123025. <https://doi.org/10.1016/J.JHAZMAT.2020.123025>

886 Tayebi-Khorami, M., Edraki, M., Corder, G., Golev, A., 2019. Re-thinking mining
887 waste through an integrative approach led by circular economy aspirations.
888 Minerals. <https://doi.org/10.3390/min9050286>

889 Tekin, G., Ersöz, G., Atalay, S., 2022. Photo-degradation of sugar processing
890 wastewater by copper doped bismuth oxyiodide: Assessment of treatment
891 performance and kinetic studies. J Environ Manag 318.
892 <https://doi.org/10.1016/j.jenvman.2022.115432>

893 Texeira, L., Calisaya-Azpilcueta, D., Cruz, C., Botero, Y.L., Cisternas, L.A., 2023.
894 Impact of the use of seawater on acid mine drainage from mining wastes. J
895 Clean Prod 383. <https://doi.org/10.1016/j.jclepro.2022.135516>

896 Thomas, S., Rayaroth, M.P., Menacherry, S.P.M., Aravind, U.K., Aravindakumar,
897 C.T., 2020. Sonochemical degradation of benzenesulfonic acid in aqueous
898 medium. Chemosphere 252, 126485.
899 <https://doi.org/10.1016/J.CHEMOSPHERE.2020.126485>

900 Vega, A.S., Arce, G., Rivera, J.I., Acevedo, S.E., Reyes-Paecke, S., Bonilla, C.A.,
901 Pastén, P., 2022. A comparative study of soil metal concentrations in Chilean
902 urban parks using four pollution indexes. Appl Geochem 141, 105230.
903 <https://doi.org/10.1016/J.APGEOCHEM.2022.105230>

904 Wang, J., Wang, S., 2020. Reactive species in advanced oxidation processes:
 905 Formation, identification and reaction mechanism. Chem Eng J 401, 126158.
 906 <https://doi.org/10.1016/J.CEJ.2020.126158>

907 Wdowczyk, A., Koc-Jurczyk, J., Jurczyk, Ł., Szymańska–Pulikowska, A., Gałka, B.,
 908 2025. Removal of selected pollutants from landfill leachate in the vegetation-
 909 activated sludge process. Waste Manag 195, 209–219.
 910 <https://doi.org/10.1016/J.WASMAN.2025.02.007>

911 Welter, J.B., Soares, E.V., Rotta, E.H., Seibert, D., 2018. Bioassays and Zahn-
 912 Wellens test assessment on landfill leachate treated by photo-Fenton process.
 913 J Environ Chem Eng 6, 1390–1395.
 914 <https://doi.org/10.1016/J.JECE.2018.01.059>

915 Yang, H., Wang, X., Wang, J., Liu, H., Jin, H., Zhang, J., Li, G., Tang, Y., Ye, C.,
 916 2025. High-value utilization of agricultural waste: A study on the catalytic
 917 performance and deactivation characteristics of iron-nickel supported biochar-
 918 based catalysts in the catalytic cracking of toluene. Energy 323, 135806.
 919 <https://doi.org/10.1016/J.ENERGY.2025.135806>

920 Yin, X., Lai, Y., Zhang, X., Zhang, T., Tian, J., Du, Y., Li, Z., Gao, J., 2025. Targeted
 921 Sonodynamic Therapy Platform for Holistic Integrative Helicobacter pylori
 922 Therapy. Adv Sci 12. <https://doi.org/10.1002/advs.202408583>

923 Youssef, M.A., El-Naggar, M.R., Ahmed, I.M., Attallah, M.F., 2021. Batch kinetics of
 924 ¹³⁴Cs and ¹⁵²⁺¹⁵⁴Eu radionuclides onto poly-condensed feldspar and perlite
 925 based sorbents. J Hazard Mater 403, 123945.
 926 <https://doi.org/10.1016/J.JHAZMAT.2020.123945>

927 Zhang, R., Schippers, A., 2022. Stirred-tank bioleaching of copper and cobalt from
 928 mine tailings in Chile. Miner Eng 180, 107514.
 929 <https://doi.org/10.1016/J.MINENG.2022.107514>

930